Improved extraction of the weak mixing angle from recent CMS forward-backward asymmetry measurements at 13 TeV with additional PDF constraints from W and Z measurements

Arie Bodek[1], Hyon-San Seo[1], and Un-Ki Yang[2]

[1] *Department of Physics and Astronomy, University of Rochester, Rochester, NY 14627, USA*
[2] *Department of Physics and Astronomy, Seoul National University, Seoul 151-747, Korea*

Presented by Hyon-San Seo at the 32nd International Symposium on Lepton Photon Interactions at High Energies,
Madison, Wisconsin, USA, August 25–29, 2025

Abstract

We present an improved extraction of the effective leptonic weak mixing angle, $\sin^2\theta^\ell_{\rm eff}$, based on the published CMS measurement of the forward–backward asymmetry ($A_{\rm FB}$) in Drell–Yan dilepton production at a center-of-mass energy of 13 TeV. The published CMS extraction already reduces parton distribution function (PDF) uncertainties by profiling with the dilepton mass dependence of $A_{\rm FB}$, yet the total uncertainty remains dominated by PDFs. We further reduce the PDF uncertainty by extending the profiling to include additional CMS measurements of the W-boson charge asymmetry and the W/Z fiducial cross-section ratios. This extended profiling yields a substantially reduced total uncertainty, resulting in $\sin^2\theta^\ell_{\rm eff} = 0.23156\pm0.00024$, which is in excellent agreement with the Standard Model prediction of 0.23161 ± 0.00004 and constitutes the most precise single determination of $\sin^2\theta^\ell_{\rm eff}$ to date.

1 Introduction

The effective leptonic weak mixing angle ($\sin^2\theta^\ell_{\rm eff}$) is a key parameter in precision tests of the Standard Model (SM). A recent CMS 13 TeV analysis of the forward–backward asymmetry ($A_{\rm FB}$) in Drell–Yan dilepton production [1] has achieved precision comparable to electron–positron collider results. However, the CMS 13 TeV determination remains limited by uncertainties in parton distribution functions (PDFs), which dominate over statistical and experimental sources.

In this work, we improve the extraction of $\sin^2\theta^\ell_{\rm eff}$ from the published CMS measurement by profiling PDFs using additional CMS measurements of the W-boson decay lepton asymmetry [2] and the W/Z cross section ratios [3]. We first validate our implementation by reproducing the published CMS extraction in xFitter [4, 5], using the same input datasets and the same nominal PDF set, CT18Znnlo. We then extend the profiling to include these additional datasets. This results in a substantial reduction of the PDF uncertainty and yields the most precise single measurement of $\sin^2\theta^\ell_{\rm eff}$ to date.

2 Reproduction of the CMS 13 TeV analysis

As described in the CMS publication [1], the value of $\sin^2\theta^\ell_{\rm eff}$ is determined in a profiling analysis by minimizing the χ^2 function

$$\chi^2(\beta_{\rm exp},\beta_{\rm th}) = \sum_i \frac{(\sigma_i^{\rm exp} + \sum_j \Gamma_{ij}^{\rm exp}\beta_{j,\rm exp} - \sigma_i^{\rm th} - \sum_k \Gamma_{ik}^{\rm th}\beta_{k,\rm th})^2}{\Delta_i^2} + \sum_j \beta_{j,\rm exp}^2 + \sum_k \beta_{k,\rm th}^2. \quad (1)$$

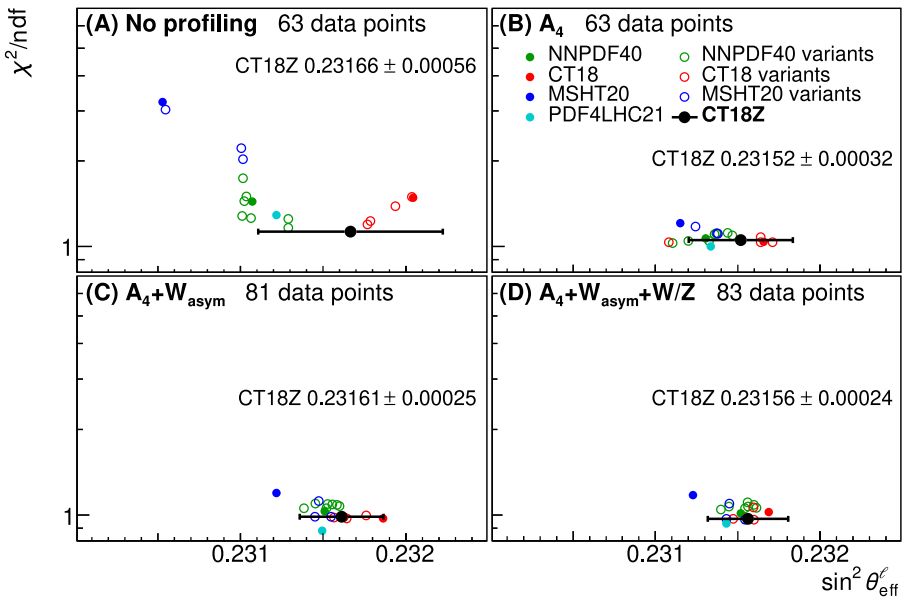

Figure 1: Extracted values of $\sin^2\theta^{\ell}_{\rm eff}$ from the 13 TeV CMS A_4 data for 19 different PDF sets on the horizontal axis. (A) Before profiling. (B) After profiling with A_4. (C) After profiling with A_4 plus W decay lepton asymmetry. (D) After profiling with A_4 plus W decay lepton asymmetry plus W/Z cross section ratios. The vertical axis shows the χ^2 values of the fits divided by the number of degrees of freedom ($N_{\rm data} - 1$), where the one degree of freedom corresponds to the free parameter $\sin^2\theta^{\ell}_{\rm eff}$.

The correlated experimental (theoretical) uncertainties are included in the nuisance vector $\beta_{\rm exp}$ ($\beta_{\rm th}$) and their impact on the measured distributions (theory predictions) is described by the matrix $\Gamma^{\rm exp}$ ($\Gamma^{\rm th}$). The index i runs over all $N_{\rm data}$ data points (63 for A_4 profiling) of the ($|y|$-M) double-differential A_4 measurement, whereas the j and k indices correspond to the experimental and theoretical uncertainty nuisance parameters, respectively. The measurements and the uncorrelated experimental uncertainties are represented by $\sigma_i^{\rm exp}$ and Δ_i, respectively, whereas the theoretical predictions are denoted by $\sigma_i^{\rm th}$. The information in the experimental covariance matrix of the double-differential A_4 measurement is included in the $\Gamma^{\rm exp}$ matrix.

The theoretical prediction is obtained with the POWHEG 2.0 event generator at multi-scale improved next-to-next-to-leading order (MiNNLO$_{\rm PS}$) accuracy in QCD [6], matched to PYTHIA 8.2 for parton showering. Photon final-state radiation is simulated with the PHOTOS 2 package [7]. In addition, next-to-leading order virtual weak corrections are included using POWHEG-Z_EW [8–10] , and the Z-boson transverse-momentum spectrum is reweighted to data, following the original CMS analysis.

The theoretical uncertainty includes contributions from the missing higher-order QCD and Electroweak (EW) corrections, as evaluated with POWHEG-Z_EW and PDF uncertainties by using grids generated at NLO with MadGraph5-aMC@nlo [11] and PineAPPL [12, 13]. The matrix $\Gamma^{\rm th}$ includes nuisance parameters reflecting the missing higher-order EW corrections, the PDF Hessian uncertainties, and the $\sin^2\theta^{\ell}_{\rm eff}$ parameter itself, which is left free in the fit. The impact of missing higher-order QCD corrections is estimated by repeating the fit for each of the six scale variations, and the maximum deviation from the central result is taken as the uncertainty.

Values of $\sin^2\theta^{\ell}_{\rm eff}$ (in units of 10^{-5}) extracted *before and after profiling* with the 13 TeV A_4 distribution are shown in Table 1 for 19 PDF sets. Most of the PDFs are Next-to-Next-to-Leading-Order QCD (NNLO), and some are Approximate-Next-to-Next-to-Next-to LO (an3lo). PDF sets labeled "qed" account for QED (Quantum Electrodynamics) effects and include photon distributions. The NNPDF40 label "mhou" indicates that these PDFs sets include corrections for "missing higher-order uncertainties". The MSHT and NNPDF PDF sets assume asymmetric sea strange quark densities. The CTEQ PDF sets (except for CT18As PDF) assume symmetric strange quark densities.

The total uncertainties in Table 1 include contributions from statistical, experimental systematic, theo-

PDF	A_4 without profiling (63 data points)			A_4 profiling (63 data points)			$A_4 + W_{\rm asym} + W/Z$ profiling (83 data points)		
	$\sin^2\theta^\ell_{\rm eff}$	Diff. from CT18Z	χ^2	$\sin^2\theta^\ell_{\rm eff}$	Diff. from CT18Z	χ^2	$\sin^2\theta^\ell_{\rm eff}$	Diff. from CT18Z	χ^2
NNPDF40									
nnlo_as_01180_hessian [14]	23107 ± 49	-59	89	23130 ± 24	-22	66	23152 ± 23	-4	83
nnlo_as_01180_qed [15]	23102 ± 46	-64	108	23144 ± 23	-8	69	23161 ± 22	5	87
nnlo_as_01180_mhou [16]	23101 ± 45	-65	79	23110 ± 27	-42	64	23145 ± 24	-11	88
nnlo_as_01180_qed_mhou [15]	23103 ± 46	-63	93	23136 ± 24	-16	69	23156 ± 23	0	88
an3lo_as_01180 [17]	23129 ± 46	-37	72	23132 ± 25	-20	65	23154 ± 23	-2	87
an3lo_as_01180_qed [17]	23129 ± 49	-37	78	23147 ± 23	-5	68	23160 ± 22	4	89
an3lo_as_01180_mhou [17]	23106 ± 47	-60	78	23120 ± 26	-32	65	23140 ± 25	-16	86
an3lo_as_01180_qed_mhou [17]	23102 ± 44	-64	90	23137 ± 23	-15	69	23156 ± 23	0	91
CTEQ									
CT18NNLO [18]	23204 ± 64	38	92	23166 ± 36	14	64	23169 ± 24	13	84
CT18Znnlo [18]	23166 ± 56	0	70	23152 ± 32	0	65	**23156 ± 24**	0	79
CT18ANNLO [18]	23179 ± 54	13	76	23164 ± 28	12	67	23160 ± 23	4	79
CT18XNNLO [18]	23194 ± 53	28	86	23171 ± 30	19	64	23160 ± 24	4	87
CT18QED-PROTON [19]	23204 ± 64	38	93	23164 ± 36	12	64	23155 ± 24	-1	80
CT18As_LatNNLO [20]	23177 ± 75	11	74	23108 ± 43	-44	64	23147 ± 35	-9	80
MSHT20									
MSHT20nnlo_as118 [21]	23053 ± 46	-113	200	23115 ± 30	-37	75	23123 ± 26	-33	96
MSHT20qed_nnlo [22]	23055 ± 59	-111	188	23124 ± 31	-28	73	23145 ± 27	-11	90
MSHT20an3lo_as118 [23]	23101 ± 47	-65	138	23138 ± 29	-14	69	23154 ± 26	-2	79
MSHT20qed_an3lo [24]	23101 ± 52	-65	126	23137 ± 31	-15	69	23143 ± 28	-13	80
PDF4LHC21_40 [25]	23122 ± 83	-44	80	23133 ± 33	-19	62	23143 ± 27	-13	77

Table 1: Values of $\sin^2\theta^\ell_{\rm eff}$ (in units of 10^{-5}) before and after profiling with the CMS 13 TeV A_4 distribution (63 points) for 19 PDF sets. Also shown are the values extracted by including the CMS 13 TeV W-decay lepton asymmetry and the CMS W/Z cross section ratios (total of 83 points) in the profiling. The total uncertainties include contributions from statistical, experimental systematic, theoretical and PDF sources. The column marked "Diff. from CT18Z" is the difference from $\sin^2\theta^\ell_{\rm eff}$ extracted with the CT18ZNNLO PDF set. Note, the χ^2 values before profiling do not include PDF errors, while the χ^2 values after profiling include PDF errors.

retical, and PDF sources. The differences in the results obtained with the various PDF sets (*before profiling*) largely reflect variations in input datasets, parameterization choices, and flavor assumptions. If there are sufficient parameters in the PDF sets, then the profiled PDFs should be able to describe all data that are used in the $\sin^2\theta^\ell_{\rm eff}$ profiling analysis with good χ^2. The columns labeled marked "Diff. from CT18Z" show the difference between the value of $\sin^2\theta^\ell_{\rm eff}$ extracted with each of the 19 PDF sets and that obtained using the nominal CT18ZNNLO PDF set.

For the nominal CT18ZNNLO set, the profiled value obtained from the 13 TeV A_4 data alone is in very good agreement with the published CMS result (Table 1), which validates our implementation of the CMS analysis in xFITTER.

3 Extended Profiling with W Charge Asymmetry and W/Z Cross Section Ratios

The uncertainty in $\sin^2\theta^\ell_{\rm eff}$ is significantly reduced after profiling with A_4, but some differences between PDF sets remain. As shown in [26], including the W-boson charge asymmetry measurements ($W_{\rm asym}$) in the profiling provides additional constraints on the d/u ratio, leading to a further reduction of the PDF uncertainty in $\sin^2\theta^\ell_{\rm eff}$. Moreover, some CT18 PDF sets lack sufficient constraints on the strange-quark distribution at high energy scales, resulting in systematically lower strange-quark densities compared to other PDFs and thereby predicting a larger effective weak mixing angle. Incorporating the W/Z cross section ratios can provide further constraints on the strange-quark distribution, helping to reduce these discrepancies.

Therefore, we perform an updated analysis of the published CMS 13 TeV A_4 data (63 data points). We also include the recent CMS $W_{\rm asym}$ measurement [2] at 13 TeV (18 additional data points) and the CMS measurements of the W and Z fiducial cross-section ratios [3] at 5.02 TeV ($12.505 \pm 0.037_{\rm stat} \pm 0.032_{\rm syst}$) and 13 TeV ($12.078 \pm 0.028_{\rm stat} \pm 0.032_{\rm syst}$), contributing 2 additional data points. The results are shown in the columns of Table 1 and in Figure 1.

Extracted values of $\sin^2\theta^\ell_{\rm eff}$ from the 13 TeV CMS A_4 data for different PDF sets are shown on the horizontal axis of each of the four panels in Fig. 1. The vertical axis shows the values of χ^2 normalized to the number of degrees of freedom, ndf $= \mathrm{N_{data}} - 1$, where the subtraction accounts for the single free parameter $\sin^2\theta^\ell_{\rm eff}$. Shown are the values before profiling (panel A, 63 data points). After profiling with A_4 (panel B, 63 data points), after profiling with A_4 and also with W decay lepton asymmetry (panel C, 81 data points), and after profiling with A_4 and the W decay lepton asymmetry and also the W/Z cross section ratios (panel D, 83 data points).

As seen in Table 1 and Figure 1, after A_4 profiling the error in the extracted value of $\sin^2\theta^\ell_{\rm eff}$ with the nominal CT18ZNNLO PDF set is reduced from 0.00056 to 0.00032. By also including the W decay lepton asymmetry and the W/Z cross section ratios the uncertainty for the nominal CT18ZNNLO is reduced to 0.00024.

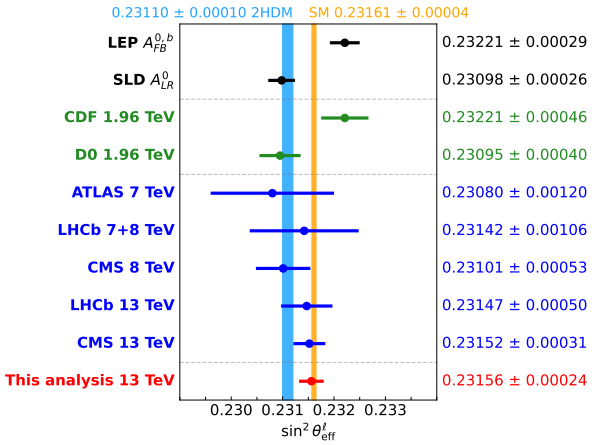

Figure 2: Comparison of $\sin^2\theta^\ell_{\rm eff}$ extracted in this analysis (labeled "This analysis 13 TeV") with previous measurements [1, 27–33] and the prediction of the 2025 SM global fit [34, 35]. Also shown is the prediction of the Two Higgs Doublet Model [36] corresponding to the CDF M_W value [37] (80.4335 ±0.0094 GeV).

Profiling with all three measurements leads to a substantial convergence across PDF sets. After profiling, the central values for 18 out of 19 PDF sets (including three of the four MSHT20 PDFs sets) lie within one standard deviation of the CT18ZNNLO result. The single profiled MSHT20 PDF set whose central value is 1.38 standard deviations low (MSHT20NNLO_AS118) has a poor χ^2. In contrast, as shown in Table 1, the profiled $MSHT20an3lo\_as118$ gives the same $\sin^2\theta^\ell_{\rm eff}$ as CT18ZNNLO with good χ^2. *By including the W decay lepton asymmetry and the W/Z cross section ratios, the differences become negligible in the extracted values of* $\sin^2\theta^\ell_{\rm eff}$ *between PDFs with asymmetric and symmetric strange quark distributions.*

Figure 2 shows a comparison of $\sin^2\theta^\ell_{\rm eff}$ extracted in this analysis with the nominal CT18ZNNLO PDF set (Labeled "This analysis 13 TeV") to previous measurements [1, 27–33]. Also shown are the predictions of the 2025 SM global fit [34, 35] and the prediction of the Two Higgs Doublet Model [36] assuming the CDF M_W value [37] of 80.4335 ±0.0094 GeV.

4 Conclusion

In conclusion, by including the new CMS 13 TeV W-boson decay lepton asymmetry and the W/Z cross-section ratios in the profiling analysis, we extract the most precise single measurement to date [38] of $\sin^2\theta^\ell_{\rm eff} = 0.23156 \pm 0.00024$. After profiling with the CMS 13 TeV A_4, $W_{\rm asym}$ and the W/Z cross section ratios, the extracted values of $\sin^2\theta^\ell_{\rm eff}$ for 18 PDF sets are within one standard deviation of the nominal CT18ZNNLO value. The value is in excellent agreement with the Standard Model value of $\sin^2\theta^\ell_{\rm eff} = 0.23161 \pm 0.00004$.

Research supported by the U.S. Department of Energy under University of Rochester grant number DE-SC0008475 and by MSIP and NRF (Republic of Korea).

References

[1] Aram Hayrapetyan et al. Measurement of the Drell-Yan forward-backward asymmetry and of the effective leptonic weak mixing angle in proton-proton collisions at $\sqrt{s} = 13$ TeV. *Phys. Lett. B*, 866:139526, 2025.

[2] Albert M Sirunyan et al. Measurements of the W boson rapidity, helicity, double-differential cross sections, and charge asymmetry in pp collisions at $\sqrt{s} = 13$ TeV. *Phys. Rev. D*, 102(9):092012, 2020.

[3] Aram Hayrapetyan et al. Measurement of the inclusive cross sections for W and Z boson production in proton-proton collisions at $\sqrt{s} = 5.02$ and 13 TeV. *JHEP*, 04:162, 2025.

[4] S. Alekhin et al. HERAFitter. *Eur. Phys. J. C*, 75:304, 2015.

[5] S. Camarda et al. QCD analysis of W- and Z-boson production at Tevatron. *Eur. Phys. J. C*, 75:458, 2015.

[6] Pier Francesco Monni, Emanuele Re, and Marius Wiesemann. MiNNLO$_{PS}$: optimizing $2 \to 1$ hadronic processes. *Eur. Phys. J. C*, 80(11):1075, 2020.

[7] Piotr Golonka and Zbigniew Was. PHOTOS Monte Carlo: A Precision tool for QED corrections in Z and W decays. *Eur. Phys. J. C*, 45:97–107, 2006.

[8] Mauro Chiesa, Fulvio Piccinini, and Alessandro Vicini. Direct determination of $\sin^2\theta^{\ell}_{eff}$ at hadron colliders. *Phys. Rev. D*, 100(7):071302, 2019.

[9] Mauro Chiesa, Clara Lavinia Del Pio, and Fulvio Piccinini. On electroweak corrections to neutral current Drell–Yan with the POWHEG BOX. *Eur. Phys. J. C*, 84:539, 2024.

[10] Luca Barze, Guido Montagna, Paolo Nason, Oreste Nicrosini, Fulvio Piccinini, and Alessandro Vicini. Neutral current Drell-Yan with combined QCD and electroweak corrections in the POWHEG BOX. *Eur. Phys. J. C*, 73(6):2474, 2013.

[11] J. Alwall, R. Frederix, S. Frixione, V. Hirschi, F. Maltoni, O. Mattelaer, H. Shao, T. Stelzer, P. Torrielli, and M. Zaro. The automated computation of tree-level and next-to-leading order differential cross sections, and their matching to parton shower simulations. *JHEP*, 07:079, 2014.

[12] Christopher Schwan. PineAPPL: NLO EW corrections for PDF processes. *SciPost Phys. Proc.*, 8:079, 2022.

[13] S. Carrazza, E. R. Nocera, C. Schwan, and M. Zaro. PineAPPL: combining EW and QCD corrections for fast evaluation of LHC processes. *JHEP*, 12:108, 2020.

[14] Richard D. Ball et al. The path to proton structure at 1% accuracy. *Eur. Phys. J. C*, 82(5):428, 2022.

[15] Richard D. Ball et al. Photons in the proton: implications for the LHC. *Eur. Phys. J. C*, 84(5):540, 2024.

[16] Richard D. Ball et al. Determination of the theory uncertainties from missing higher orders on NNLO parton distributions with percent accuracy. *Eur. Phys. J. C*, 84:517, 2024.

[17] Richard D. Ball et al. The path to N^{3}LO parton distributions. *Eur. Phys. J. C*, 84(7):659, 2024.

[18] Tie-Jiun Hou et al. New CTEQ global analysis of quantum chromodynamics with high-precision data from the LHC. *Phys. Rev. D*, 103(1):014013, 2021.

[19] Keping Xie, Bei Zhou, and T. J. Hobbs. The photon content of the neutron. *JHEP*, 04:022, 2024.

[20] Tie-Jiun Hou, Huey-Wen Lin, Mengshi Yan, and C. P. Yuan. Impact of lattice strangeness asymmetry data in the CTEQ-TEA global analysis. *Phys. Rev. D*, 107:076018, 2023.

[21] S. Bailey, T. Cridge, L. A. Harland-Lang, A. D. Martin, and R. S. Thorne. Parton distributions from LHC, HERA, Tevatron and fixed target data: MSHT20 PDFs. *Eur. Phys. J. C*, 81(4):341, 2021.

[22] T. Cridge, L. A. Harland-Lang, A. D. Martin, and R. S. Thorne. QED parton distribution functions in the MSHT20 fit. *Eur. Phys. J. C*, 82(1):90, 2022.

[23] J. McGowan, T. Cridge, L. A. Harland-Lang, and R. S. Thorne. Approximate N^{3}LO parton distribution functions with theoretical uncertainties: MSHT20aN^{3}LO PDFs. *Eur. Phys. J. C*, 83(3):185, 2023. [Erratum: Eur.Phys.J.C 83, 302 (2023)].

[24] Thomas Cridge, Lucian A. Harland-Lang, and Robert S. Thorne. Combining QED and approximate N^{3}LO QCD corrections in a global PDF fit: MSHT20qed_an3lo PDFs. *SciPost Phys.*, 17(1):026, 2024.

[25] Richard D. Ball et al. The PDF4LHC21 combination of global PDF fits for the LHC Run III. *J. Phys. G*, 49:080501, 2022.

[26] A. Bodek, J. Han, A. Khukhunaishvili, and W. Sakumoto. Using Drell-Yan forward-backward asymmetry to reduce PDF uncertainties in the measurement of electroweak parameters. *Eur. Phys. J. C*, 76(3):115, 2016.

[27] S. Schael et al. Precision electroweak measurements on the Z resonance. *Phys. Rept.*, 427:257–454, 2006.

[28] Timo Antero Aaltonen et al. Measurement of $\sin^2\theta^{\rm lept}_{\rm eff}$ using e^+e^- pairs from γ^*/Z bosons produced in $p\bar{p}$ collisions at a center-of-momentum energy of 1.96 TeV. *Phys. Rev. D*, 93(11):112016, 2016. [Addendum: Phys.Rev.D 95, 119901 (2017)].

[29] Victor Mukhamedovich Abazov et al. Measurement of the Effective Weak Mixing Angle in $p\bar{p} \to Z/\gamma^* \to \ell^+\ell^-$ Events. *Phys. Rev. Lett.*, 120(24):241802, 2018.

[30] Georges Aad et al. Measurement of the forward-backward asymmetry of electron and muon pair-production in pp collisions at $\sqrt{s} = 7$ TeV with the ATLAS detector. *JHEP*, 09:049, 2015.

[31] Albert M. Sirunyan et al. Measurement of the weak mixing angle using the forward-backward asymmetry of Drell-Yan events in pp collisions at $\sqrt{s} = 8$ TeV. *Eur. Phys. J. C*, 78(9):701, 2018.

[32] Roel Aaij et al. Measurement of the forward-backward asymmetry in $Z/\gamma^* \to \mu^+\mu^-$ decays and determination of the effective weak mixing angle. *JHEP*, 11:190, 2015.

[33] R. Aaij et al. Measurement of the effective leptonic weak mixing angle. *JHEP*, 12:026, 2024.

[34] S. Navas et al. Review of particle physics. *Phys. Rev. D*, 110(3):030001, 2024.

[35] S. Navas et al. Review of particle physics 2025 online update, 2025.

[36] Thomas Biekötter, Sven Heinemeyer, and Georg Weiglein. Excesses in the low-mass Higgs-boson search and the W-boson mass measurement. *Eur. Phys. J. C*, 83(5):450, 2023.

[37] T. Aaltonen et al. High-precision measurement of the W boson mass with the CDF II detector. *Science*, 376(6589):170–176, 2022.

[38] Arie Bodek, Hyon-San Seo, and Un-Ki Yang. Precision Measurements of the Electroweak Mixing Angle in the Region of the Z pole. 8 2025. arXiv:2508.18022 (to be published in Physics Reports).